

# Investigating the variation in mechanical properties of hybrid nanoparticle reinforced A390 hypereutectic Al-Si alloy

M Iskander<sup>1</sup>, I El-Mahallawi<sup>1,2</sup> and M EL Shazly<sup>3</sup>

<sup>1</sup> Faculty of Engineering, Department of Mechanical Engineering, The British University in Egypt, El-Sherouk City, Cairo 11837, Egypt

<sup>2</sup> Mining, Petroleum and Metallurgical Engineering Dept., Faculty of Engineering, Cairo University, Giza, 12613, Egypt

<sup>3</sup> Department of Mechanical Design and Production Engineering, Faculty of Engineering, Cairo University, Giza, 12613, Egypt

Corresponding Email: [mark.safwat@bue.edu.eg](mailto:mark.safwat@bue.edu.eg)

**Abstract.** A390 hyper-eutectic Al-Si alloy is fabricated as monolithic alloy and with different percentages of nano-reinforcements added to the alloy through stir casting with (1% ZrO<sub>2</sub>), (0.5% ZrO<sub>2</sub> with 0.5% TiO<sub>2</sub>), (0.5% ZrO<sub>2</sub> with 1.5% Al<sub>2</sub>O<sub>3</sub>), (1% ZrO<sub>2</sub> with 1% Al<sub>2</sub>O<sub>3</sub>) and (1.5% ZrO<sub>2</sub> and 0.5% Al<sub>2</sub>O<sub>3</sub>). Mechanical and microstructural properties were investigated along with SEM and mapping images. The results show significant refinement across all specimens of 72% in primary silicon size, 82% in dendritic arm length and 59% reduction in dendritic arm spacing. Results also show great improvement in most specimens up to 90% in tensile strength, up to 16% hardness and around 2% enhancement in elongation. However, a great scatter in the results is present in the mechanical properties proving the challenge in the repeatability of the alloys through traditional stir casting manufacturing methods. SEM and EDX analyses confirmed non-homogeneous nanoparticle distribution in some specimens, while the presence of Al<sub>3</sub>Zr intermetallic phases contributed to enhanced strength and reduced defects. This work provides insights into the strengthening mechanisms and fabrication challenges of hybrid nanoparticle-reinforced Al-Si alloys for various applications.

## 1. Introduction

One of the pivotal shifters in the modern industry and played a crucial role in the advancements of automotive, construction and electronics industry was the introduction of aluminum alloys. Aluminum alloys have a rich history dating back to the 19<sup>th</sup> century as its production method became more economical by the introduction of the Hall-Héroult process, one of the corner stones in the advancement of modern metallurgy [1]. Prior to the Hall-Héroult process, aluminum was used extensively in aerospace applications from the 2xxx series to the 7xxx series and is still majorly used in the same applications and more. Its significance can be shown by the attractive properties it presents, for instance, it offers a light-

weight structure with high strength to weight ratio implemented in various sectors interested in reducing fuel consumption and optimizing its design [2]. In addition, aluminum is highly recyclable, corrosion resistant and ductile. Despite all, aluminum alone without any advancements in manufacturing to strengthen will prove to be trivial, there are many developments in aluminum alloys such as heat treatment, nano-reinforcements and additive manufacturing. One effective method of heat treatment, precipitation hardening, it is done by three main process solid solution treatment that focuses on the dissolvment of the alloying elements inside the matrix, afterwards, quenching the alloy to maintain the supersaturated condition and finally aged at lower temperatures to introduce fine and hard precipitates of the second phase to hinder the dislocation movement.

Nanoparticles significantly enhance the mechanical and physical properties of metallic composites through grain refinement, thermal stability, and dispersion strengthening. Grain refinement induced by nanoparticles is effective by restricting the nucleation process during solidification resulting in higher grain count and finer grain structure, in return, an improvement in strength and hardness is noticed because of the Hall-Patch effect [3]. A study conducted by Zhang et al., concluded that the implementation of SiC nanoparticles to aluminum, reduced grain size to almost 50% and therefore increasing its mechanical properties [4]. Thermal stability is crucial for applications with elevated temperatures like engines and turbines, for the metallic composite to retain its mechanical properties at temperatures where it usually fades. Ezatpour HR. et al., studied the effect of adding  $Al_2O_3$  nanoparticles to aluminum 6061 and found that reinforcement increased the activation energy for deformation at temperatures up to 500 °C, hence making it a powerful candidate for high temperature applications [5]. Another important mechanism, Dispersion Strengthening, a mechanism that involves other mechanism such as Orowan and Particle Shearing mechanisms. The difference in both mechanisms can be shown in figure 1 and is controlled by the particle size where a relatively small particle size will induce a particle shearing mechanism unlike a large particle size that will encourage Orowan or bowing mechanism.

There are various methods for the production of nano-reinforced alloys such as stir casting and rheo casting however, the repeatability of such experiments may prove too hard for multiple fabrication process due to multiple factors. Thus far, limited analysis has been conducted on the A390 alloy reinforced with nanoparticles using stir casting method whilst achieving consistent mechanical properties due to factors such as non-uniform dispersion and porosity. This study aims to investigate the influence of different types and combinations of nanoparticles on the mechanical properties and microstructure of A390 alloy, as well as the challenges associated with achieving repeatability using the traditional stir casting process.

## **2. Methodology**

### *2.1 Materials used*

The base metal used in this paper was Aluminum 390 hypereutectic Al-Si Alloy with its chemical compositions shown in table 1, this alloy is heavily utilized in aerospace and automotive applications. In addition, the nanoparticles used in this research were  $Al_2O_3$ ,  $TiO_2$  and  $ZrO_2$  acquired from (Nano Gate Company) and characteristics of reinforcements attached in table 2, nanoparticles were analyzed as shown in figure 1 using TEM performed on JEOL JEM-2100 high resolution transmission electron microscope at an accelerating voltage of 200 kV. All nano-reinforcements were encapsulated inside a thin and small size sheet of aluminum foil.

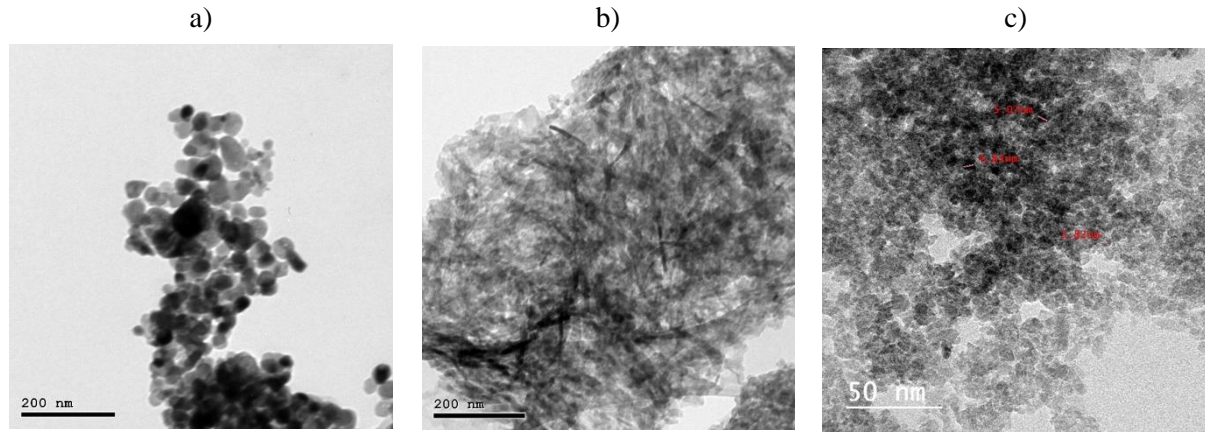


**Figure 1.** a)  $ZrO_2$ , b)  $Al_2O_3$  & c)  $TiO_2$  TEM images

**Table 1.** A 390 Chemical Composition

Chemical Composition (%)								
Alloy	Si	Mg	Fe	Cu	Ti	Zn	Mn	Al
A390	17	0.45	0.5	4.5	0.2	0.1	0.1	Bal.

**Table 2.** Nano-particles Characterization

Reinforcements	$ZrO_2$	$Al_2O_3$	$TiO_2$
Density ( $g/cm^3$ )	5.89	3.6	4.23
Particle Size (nm)	30	<50	<10
Shape	Spherical	Spherical	Spherical
Crystal Structure	Tetragonal	FCC	Tetragonal
Appearance	White	White	Grayish

## 2.2 Fabrication Tools & Methods

An electric furnace with a control unit and thermocouple to monitor and control the desired temperature with a manually lifted graphite crucible with a maximum capacity of 8 kg. charge. In addition, an external mixing method was fabricated for this experiment consisting of a drill that had an extended stainless-steel shaft with an impeller mounted at the end of it, the drill had an rpm of 350. Afterwards, aluminum mixture is degassed by using Argon gas to avoid any casting defects arising from gas entrapped in the mixture and poured into a cast-iron mold with 20 mm Diameter and 150 mm in height for each specimen inside the mold.

A charge of 600 grams of A390 ingot pieces was placed inside the furnace and heated to a temperature of 780 °C for each condition to exceed aluminum melting point and take into consideration the temperature drop from stirring and degassing with argon. Subsequently, different percentages and conditions of nanoparticles shown in table (3) are capsulated and pre-heated to 300 °C to avoid any agglomerations that could ruin the experiment. The molten aluminum is then lifted manually from the oven, capsules dropped and mixed carefully at a speed of 350 rpm for 1 minute & 30 seconds for a

suitable dispersion of nanoparticles, to be degassed with argon for 25 seconds. Mixture achieved a pouring temperature ranging between 610 – 630 °C. Finally, the semi-solid-state aluminum was poured into the die cast and experiment repeated for each condition. Despite all efforts to minimize errors, achieving constant pouring temperature, constant stirring and degassing time, there were some nuisance factors out of the researchers control such as the time from removing the crucible to pouring, angle of stirring and pouring velocity.

**Table 3.** Experiment Conditions

Group Name	Condition
A390	Aluminum without reinforcements
A390 1Z	Reinforced with 1% ZrO <sub>2</sub>
A390 0.5Z/1.5A	Reinforced with 0.5% ZrO <sub>2</sub> & 1.5 % Al <sub>2</sub> O <sub>3</sub>
A390 1.5Z/0.5A	Reinforced with 1.5% ZrO <sub>2</sub> & 0.5 % Al <sub>2</sub> O <sub>3</sub>
A390 1Z/1A	Reinforced with 1% ZrO <sub>2</sub> & 1% Al <sub>2</sub> O <sub>3</sub>
A390 0.5Z/0.5T	Reinforced with 0.5% ZrO <sub>2</sub> & 0.5% TiO <sub>2</sub>

### 2.3 Testing Methods

The tests done to investigate and characterize the fabricated material were tensile, microstructure, microhardness, SEM and EDX tests, each condition had 3 replicates for all mechanical tests. Tensile tests were performed on (ibertest testcom 100) and done according to the E8M standard, the tests were conducted with a strain rate of 2 mm/min. The specimens for microstructure were cut into 3 cm height cylindrical parts and flattened on a turning machine. Microstructure tests were prepared by grinding with SiC fine sandpapers (180, 320, 600, 800, 1200, 2400, 4000) to ensure even surface preparation for microscopy. After grinding, the specimens were polished for 10 minutes using a 0.3 µm Alumina suspension. Subsequently, they were etched with Keller's reagent for 30 seconds, washed, and dried. Finally, the specimens were examined under an optical microscope to capture their microstructures and measure the size of primary silicon, secondary dendritic arm length and dendritic arm spacing through (ImageJ, National Institute of Health, USA). Another main test, a hardness Vickers test (HV1) was fulfilled with a load of 1 kg and a dwell time of 15 seconds after microstructure preparation, using Q-ness 60M machine. Furthermore, the investigation on the homogeneity of the nano-reinforcements and the presence of any foreign elements was done using a Quanta FEG 250 NRC accompanied with EDX test.

## 3. Results and Discussion

### 3.1 Analysis of Mechanical Properties

The data obtained shown in figure 2 shows the scattering of tensile strength, elongation and hardness experiments. The data for the tensile strength ranged from 75 MPa to 232 MPa, these values are greatly scattered with the lowest decrease of 40% in the A390 0.5Z/0.5T alloy that may have occurred due to defects such as porosity that is common in gravity die casting method and agglomeration of nanoparticles inside the composite [6]. Furthermore, figure 3 shows SEM & EDX mapping for one of the specimens with the rectangular area on the right with no zirconia present whilst mapping the whole image on the left, zirconia can be observed inside the highlighted circular area as purple dots, showing non homogenous distribution of nanoparticles concentrated on the left region alone.

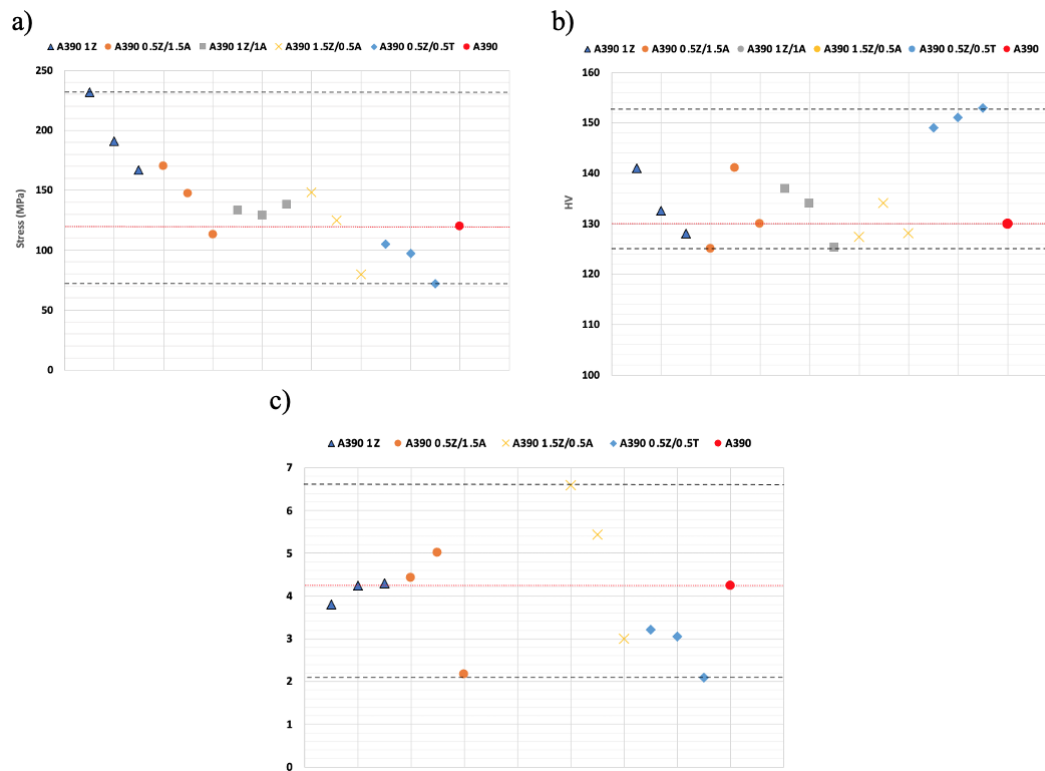


**Figure 2.** Scatter Plot of a) Tensile Strength b) Hardness c) Elongation

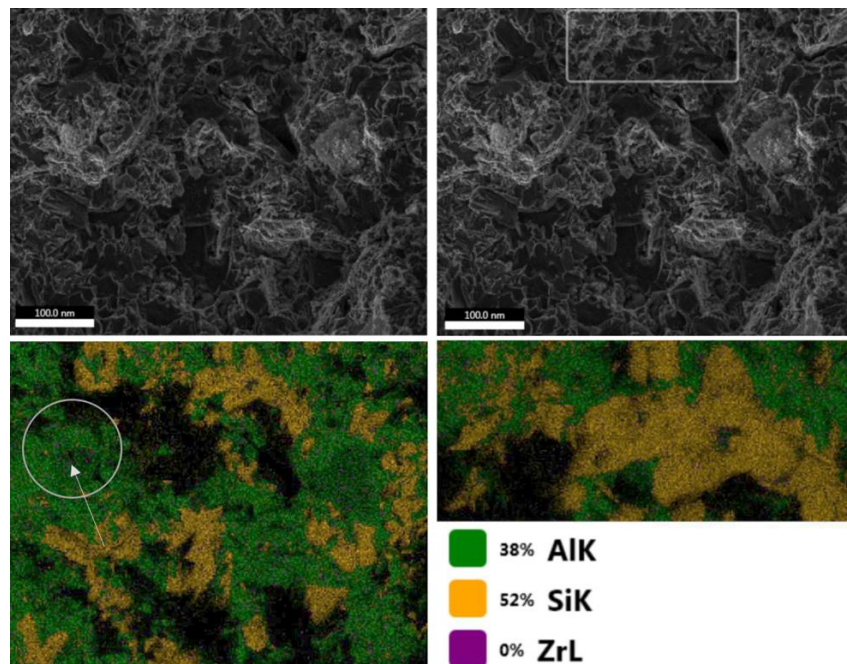


**Figure 3.** (A390 0.5Z/1.5A) SEM and Mapping for non-homogenous distribution

On the other hand, introducing zirconia and alumina nano particles both in hybrid conditions and zirconia alone improved tensile strength by more than 90%, this may have occurred due to several strengthening mechanisms such as load transfer from the matrix to the nano-reinforcements, Orvan mechanism and dispersion strengthening due to proper dispersion of the nano-reinforcements which can be proved from figure 4 showing the dispersion of zirconia [7, 8] . For the hardness it ranged from 125 HV to 153 HV and for the elongation the data ranged from 2.2% to 6.6%. As shown in table 4, Choi H et al. concluded that there was a significant enhancement in the mechanical properties yielding a strength of 154 MPa and ductility of 1.72% when introducing 0.5%  $\text{Al}_2\text{O}_3$  via ultra-sonic cavitation method [9]. In addition, El Mahallawi et. al determined that the addition of 2%  $\text{Al}_2\text{O}_3$  with a pouring temperature of 620 to 640 °C by stir casting method, caused strength to rise to 167 MPa and ductility to 3% [10]. Finally, Mohamadigangaraj et al. investigated the influence of various processing parameters on the fabrication of A390 alloy reinforced with 10% micro-sized SiC particles using the stir casting method, focusing on stirring time, temperature, and speed [11]. The findings revealed that decreasing the stirring temperature while increasing both stirring time and speed significantly enhanced the mechanical properties of the alloy. Specifically, this optimization resulted in a notable increase in ultimate tensile strength to 230 MPa and ductility to 4.2%, highlighting the critical role of these parameters in improving the performance of the reinforced A390 alloy Although the data presented in figure 2 shows a that, generally, the addition of nanoparticles resulted an increase in tensile mechanical properties and hardness compared to the monolithic alloy, yet the wide scatter cannot be missed. The variation and wide range of data doesn't specifically prove the enhancement of nano-reinforcement on mechanical properties but rather the difficulty in manufacturing through traditional methods such as stir casting which may be due to various conditions such as stirring time, angle and the uniformity in the distribution of nanoparticles.

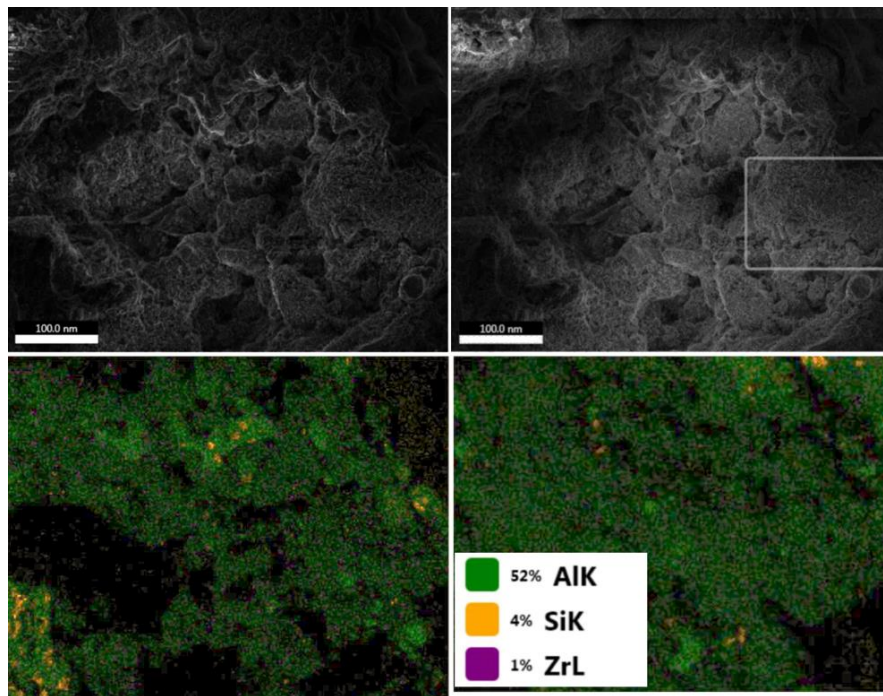


**Figure 4.** (A390 0.5Z/1.5A) SEM and Mapping for homogenous distribution

**Table 4.** Comparison between author's results and literature

Material A390	Strength (MPa)	Elongation (%)	Hardness (HV)
Author's Work	75 - 232	2.2 - 6.6	125-153
Choi H et. al [9]	122-154	0.37 - 1.72	NA
El Mahallawi I et al. [10]	NA	NA	105 - 155
El Mahallawi I et al. [11]	112 - 167	0.9 - 3	NA
Mohamadigangaraj J et al. [12]	170 - 230	2.8 - 4.2	121

### 3.2 Optical Microscope Results

The data collected from microstructure images shows shifting in the microstructure after the addition of reinforcements. Sample A390 shown in figure 5 a show the presence of the typical microstructure of A390 with equiaxed and dendritic  $\alpha$ -Al, accompanied with different irregular and regular shapes of primary silicon as well as, binary eutectic phase. The primary Silicon shown in figure 5 a demonstrates one of the main problems of traditional Al-Si cast alloys showing gaps inside the primary silicon particles which results in crack formation due to the brittle nature of silicon, therefore, the introduction of different nano-reinforcements tends to change size and shape of primary silicon, dendritic arm spacing and dendritic arm length as shown in both figure 5 & 6. The following change is a result of several nano-reinforcements acting as a heterogenous nucleating agent while other reinforcements hindering the growth of silicon phase during solidification thus refining primary silicon [10]. According to I. El-Mahallawi et al., the refining of the primary silicon phase can significantly increase the ductility of the material due to their small lattice mismatch with silicon [11]. Additionally, they influence the eutectic growth mode, modifying the structure of eutectic Si by hindering its growth and occasionally acting as nuclei during the eutectic reaction. However, the modification effect is mostly limited to the areas around primary Si particles due to the agglomeration of nanoparticles [9]. On the other hand, it can be noticed in figure 5 that several porosity spots are present which in return can significantly affect the mechanical properties of the alloy and according to Mohamadigangaraj J et al., can be controlled by different parameters such as stirring time, temperature and speed [12, 6]. Data in figure 6 was acquired through (ImageJ, National Institute of Health, USA) showing significant reduction across all alloys with A390 0.5Z/0.5T showing the greatest reduction of 72% in primary silicon size, 82% in dendritic arm length and 59% reduction in dendritic arm spacing. The primary silicon size showed almost 60% reduction in the A390 1Z specimens and almost 65% reduction in both A390 1.5Z/0.5A & 1Z/1A specimens. In addition, dendritic arm length was reduced by almost 43% in the A390 1Z/1A specimens, 56% in the A390 1Z specimens and almost 66% in the A390 1.5Z/0.5A specimens. Finally, the reduction in dendritic arm spacing averaged at almost 40% in all specimens except A390 0.5Z/0.5T. All the following results strongly correlates with research throughout the years proving the effect of nano-reinforcements on the microstructure features of Al-Si cast alloys with A390 0.5Z/0.5T showing the outstanding results.



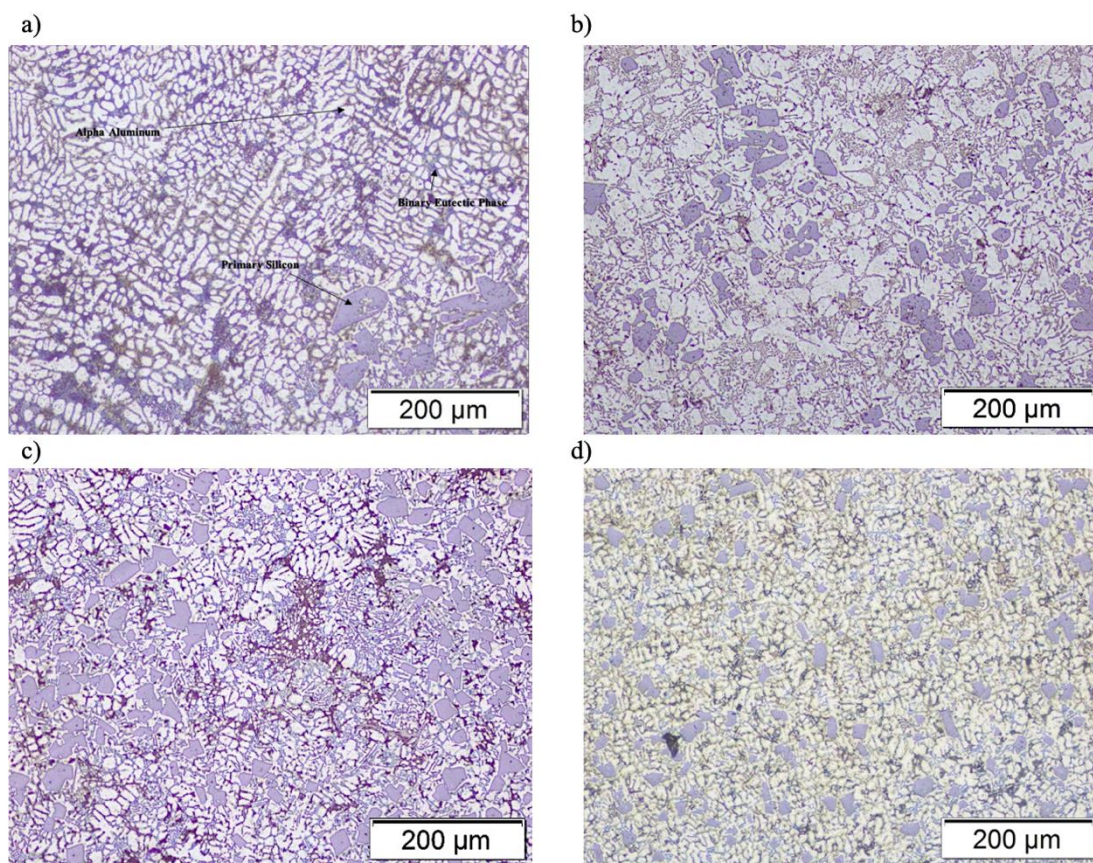


**Figure 5.** a) A390 b) A390 1.5Z/0.5A c) A390 1Z/1A d) A390 0.5Z/0.5A

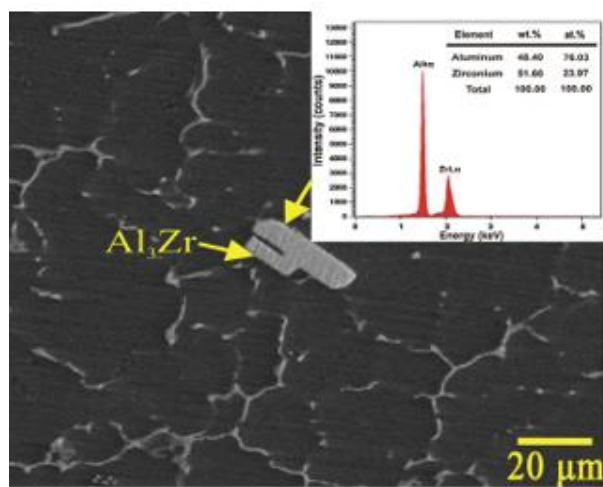


**Figure 6.** SEM and EDS tests showing  $Al_3Zr$  phase



Finally, figure 7 showed the presence of intermetallic phase of  $\text{Al}_3\text{Zr}$  which according to Long W et al., the following phase greatly reduced defects and porosity in aluminum however, as its percentage increased mechanical properties began to decline [13]. Moreover, Wang C et al., investigated the effect of  $\text{Al}_3\text{Zr}$  on ring cylinders used in space launch vehicles and concluded the effect of proper dispersion in enhancing strength and grain refinement [14].

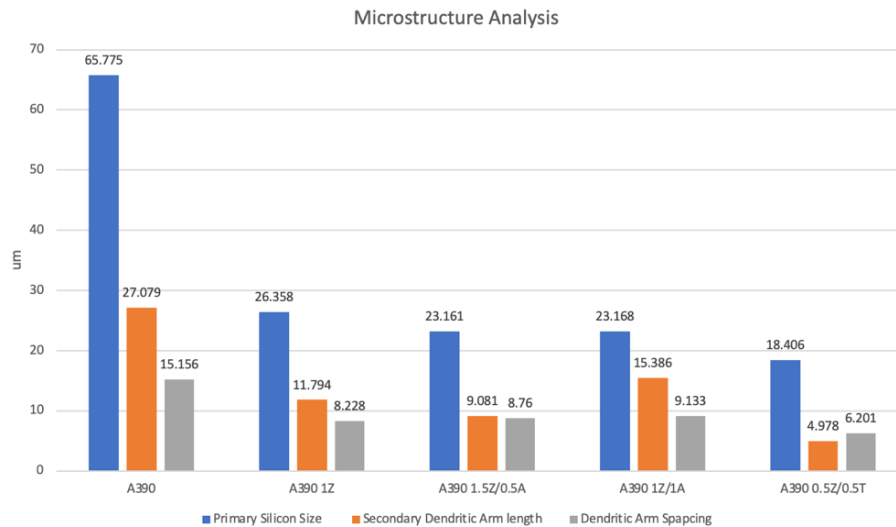


**Figure 7.** primary silicon size, dendritic arm length and spacing measurements

#### 4. Conclusion

The conducted experiments showed a significant increase of 90% in the tensile strength of A390 when reinforced with 1% Zirconia, 16 % in the hardness of the alloy reinforced with 0.5% Zirconia and 0.5% Titanium dioxide and 2% increase in ductility in the alloy reinforced with 1.5% zirconia & 0.5% Alumina. In addition, results shows significant refinement across all specimens of 72% in primary silicon size, 82% in dendritic arm length and 59% reduction in dendritic arm spacing. However, it also showed a wide variation in the data and a wide scatter due to the difficulty in reliably replicating the fabrication process. The challenge in replicating the experiment comes due to various reasons such as stirring angle, time and uniform distribution of nanoparticles which is proven with the mapping of specimens and the microstructure of the fabricated alloys. Therefore, for future work, the analysis and study of casting parameters such as stirring time, speed and temperature is needed to ensure constant and optimal mechanical properties. In addition, different fabrication methods need to be researched such as ultra-sonic cavitation method and rheo-casting.

#### References

- [1] Kaufman J 2000 Introduction to Aluminum Alloys and Tempers *ASM International*.
- [2] Miller W S, Zhuang L, Bottema J, Wittebrood A J , De Smet P, Haszler A and Vieregge A 2000 Recent development in aluminium alloys for the automotive industry *Materials Science and Engineering A-structural Materials Properties Microstructure and Processing* **280** 37-49.
- [3] Cao C, Yao G, Jiang L, Jiang L, Sokoluk M, Wang X, Ciston J, Javadi A, Guan Z, De Rosa I M, Xie W, Lavernia E J, Schoenung J M and Li X 2019 Bulk Ultrafine Grained/Nanocrystalline Metals via Slow Cooling *Science Advances*, **5**.

- [4] Zhang X & Chen Y 2019 Mechanical Properties of Al-SiC Nanocomposites *Materials Science & Technology* **6** 1027-1037.
- [5] Ezatpour H, Sajjadi S A, Chaichi A and Ebrahimi G R 2017 Mechanical and Microstructure Properties of Deformed Al–Al<sub>2</sub>O<sub>3</sub> Nanocomposite at Elevated Temperature *Journal of Materials Research* **6** 1118-1128.
- [6] John C 2003 *The Physics of Casting* Elsevier Ltd. Oxford 19-54.
- [7] Huo S, Xie L, Xiang J, Pang S, Hu F and Umer U 2018 Atomic-level Study on Mechanical Properties and Strengthening Mechanisms of Al/SiC Nano-Composites *Appl. Phys. A*. **124**.
- [8] Puspitasari P, Sasongko M, Sukarni, Murdanto P and Wahono 2019 Mechanical Properties of Al-Si Alloy with Nanoreinforced Manganese Oxide by Stir Casting Method *AIP Conf. Proc.*
- [9] Choi H, Konishi H and Li X 2011 Al<sub>2</sub>O<sub>3</sub> Nanoparticles Induced Simultaneous Refinement and Modification of Primary and Eutectic Si Particles in Hypereutectic Al–20Si Alloy *Materials Science and Engineering A* **541** 159-165.
- [10] El Mahallawi I S, Shash Y S, Rashad R M, Abdelaziz M H, Mayer J and Schwedt A 2014 Hardness and Wear Behaviour of Semi-Solid Cast A390 Alloy Reinforced with Al<sub>2</sub>O<sub>3</sub> and TiO<sub>2</sub> Nanoparticles *Arab J Sci Eng.* **39** 5171–5184.
- [11] El Mahallawi I, Othman O A, Abdelaziz M H, Raed H, Abd El-Fatah T, Ali S and Grandfield J 2014 Understanding the Role of Nanodispersions on the Properties of A390 Hypereutectic Al-Si Cast Alloy *Light Metals 2014* 1361-1365.
- [12] Mohamadigangaraj J, Nourouzi S and Jamshidi Aval H 2019 Microstructure, Mechanical and Tribological Properties of A390/SiC Composite Produced by Compocasting *Transactions of Nonferrous Metals Society of China* **29** 710-721.
- [13] Zhang W, Xu K, Long W and Zhou X 2017 Microstructure and Compressive Properties of Porous 2024Al-Al<sub>3</sub>Zr Composites *Metals* **2022** **12**.
- [14] Zhang J, Zeng H, Wang C and Tang Z 2022 Effect of Al<sub>3</sub>Zr Dispersoid on Microstructure and Mechanical Properties of Al-Cu-Li Alloy During Composite Spinning-Extrusion Forming *Frontiers in Materials* **9**.